Controlled hydrophobic modification of cellulose nanocrystals for tunable Pickering emulsions

William Dudefoi, Benjamin Dhuiège, Isabelle Capron, Gilles Sèbe

1

Controlled hydrophobic modification of cellulose nanocrystals for tunable Pickering emulsions

William Dudefoi[b], Benjamin Dhuiège[a], Isabelle Capron[b,*], Gilles Sèbe[a,*]

[a] Univ. Bordeaux, CNRS, Bordeaux INP, LCPO, UMR 5629, F-33600 Pessac, France

[b] INRAE, UR BIA, F-44316, Nantes, France

Abstract

Cellulose nanocrystals (CNC) are known to promote highly stable oil-in-water (O/W) Pickering emulsions. Our work consisted in producing CNCs with different hydrophilic/hydrophobic balance at their surface by chemical functionalization (acylation with model functional vinyl esters) and to identify the adequate conditions allowing the stabilization of direct O/W or inverse W/O Pickering emulsions. Whatever the surface degree of substitution (DS_{Surf}), CNCs grafted with linear acyl chains of 2 to 6 carbons led to the exclusive formation of direct O/W emulsions. Distinctively, both O/W and W/O emulsions could be obtained when the linear chain contained 8 carbons or more, at low and high DS_{Surf}, respectively. By adjusting the length of the grafted chain, DS_{Surf} and particles concentration, we were able to monitor the type of emulsion formed, droplet size and surface coverage at the oil/water interface.

1. Introduction

An emulsion is a system of dispersed droplets of one immiscible liquid in another, stabilized by an amphiphilic surface reactive agent composed by both a polar hydrophobic and a non-polar hydrophilic extremities. Emulsions are being used in a broad range of daily life products, such as in food industry, cosmetics, or pharmaceuticals, and in most cases, the surface active agents used are surfactants; i.e. chemical products. However, surfactants may be the cause of some undesirable adverse effects, such as skin irritation for the consumer, but also have negative impact on the environment (Belanger et al., 2006). As an alternative to chemical surfactants, emulsions can also be stabilized by the use of solid particles, forming so-called Pickering emulsions (Pickering, 1907; Arditty, Whitby, Binks, Schmitt, & Leal-Calderon, 2003). This type of emulsion also has the advantage of having an adsorption energy at the interface thousands times greater than for surfactants, leading to a better stability of the emulsion with the particles irreversibly anchored at the interface of the emulsion (Binks, 2002). Among the most interesting solid particles used for Pickering emulsions are cellulose nanocrystals (CNCs). Indeed, cellulose is a biodegradable biopolymer, main building block of trees and plants and composed of ordered crystalline regions interrupted by amorphous regions. The amorphous regions can be hydrolyzed using sulfuric acid, resulting in the production of rod-like nanocrystals decorated with sulfate half-ester groups at their surface (Habibi, Lucia, & Rojas, 2010; Moon, Martini, Nairn, Simonsen, & Youngblood, 2011). The use of unmodified CNCs as Pickering emulsion stabilizer has been first demonstrated in 2011 (Kalashnikova, Bizot, Cathala, & Capron, 2011). It was shown that unmodified CNCs dispersed in water, mixed with an apolar phase, such as hexadecane, can adsorb at the oil-water interface, preventing destabilization from coalescence for a very long period of more than one year. Small angle neutron scattering experiments carried out with a contrast variation method probed the arrangement of CNCs at the interface. These results showed that the (200)

crystalline plane of the CNCs directly interacts with the interface without deforming it (Cherhal, Cousin, & Capron, 2016). As a consequence, surface interactions occur between the CH of the CNCs and the alkyl chain of hexadecane after desorption of the aqueous layer. These performances in stabilizing oil-in-water (O/W) Pickering emulsions are reached through the formation a dense 2D interfacial network around the droplets (Kalashnikova, Bizot, Cathala, & Capron, 2012), with the possibility to control their size by varying the CNCs concentration (Capron, Rojas, & Bordes, 2017; Cherhal, Cousin, & Capron, 2016). This process generally requires the addition of salt to screen the repulsion between the negatively charged particles. In another approach, surface modification can also be carried out (Eyley & Thielemans, 2014; Habibi, 2014), to finely adjust the hydrophilic/hydrophobic balance at the surface of the CNCs. In that case, O/W (Sèbe, Ham-Pichavant, & Pecastaings, 2013; Werner, Schmitt, Sèbe, & Heroguez, 2017; Werner, Sèbe & Héroguez, 2018), water-in-oil (W/O) (Xhanari, Syverud, & Stenius, 2011; Lee, Blaker, Murakami, Heng, & Bismarck, 2014; Zhang, Tam, Wang, & Sèbe, 2018; Werner, Schmitt, Sèbe, & Héroguez, 2019) or double (Cunha, Mougel, Cathala, Berglund, & Capron, 2014) Pickering emulsions can be obtained, depending on the surface wettability of the particles.

In this work, a wide range of amphiphilic cellulose nanocrystals were prepared by acylation with model vinyl esters of various chain length and surface degree of substitution (DS_{Surf}), in order to i) investigate the impact of the surface functionalization on the properties of Pickering emulsions prepared from hexadecane, and ii) identify the adequate conditions allowing the stabilization of O/W or W/O emulsions.

2. Material and methods

2.1 Material

Cellulose nanocrystals (CNCs) were isolated by sulfuric acid treatment of wood pulp and purchased from the University of Maine. Vinyl esters (in braquets: nomenclature, degree of purity) were purchased from Sigma Aldrich or TCI suppliers and not further purified before use: vinyl acetate (VA, 99%, Sigma), vinyl propionate (VPro, 98%, Sigma), vinyl butyrate (VBut, 98%, TCI), vinyl hexanoate (VHex, 99%, TCI), vinyl n-octanoate (VOct, 99%, TCI), vinyl decanoate (VDec, 99%, TCI), vinyl laurate (VLau, 99%, TCI), Vinyl myristate (VMyr, 99%, TCI), vinyl palmitate (VPalm, 96%, TCI) and vinyl stearate (VSte, 95%, TCI). Potassium carbonate (K_2CO_3), dimethylsulfoxide (DMSO), tetrahydrofuran (THF), toluene, hexadecane, fluorescein, technical acetone and ethanol were purchased from Sigma Aldrich. DMSO and K_2CO_3 were systematically dried beforehand: on 5-Å molecular sieve for DMSO; in an oven at 50°C for K_2CO_3 (overnight).

2.2 Chemical functionalization of the CNCs

After weighing 2.5 g of CNCs and 1.0 g of K_2CO_3 in a double-necked 150 mL flask, 100 mL of dried DMSO was added and the solution was sonicated for 1 min (Bandelin, MS72 probe, 1.5 kJ). The volume of vinyl ester added was calculated for each treatment, to fit the molar ratio $N_{vinyl\ ester}/N_{OHs} = 3.75$, with N_{OHs} corresponding to the number of OH groups available at the surface of the CNCs (estimated at 3.1 mmol.g^{-1} in Brand, Pecastaings, & Sèbe, 2017). After introduction of the vinyl ester, the mixture was heated in an oil bath sustained at 80°C, and magnetically stirred at 250 rpm for 5h. The reaction medium was then sampled at different periods of time (10 min, 15 min, 30 min, 45 min, 1h, 2h, 3h, 4h or 5h). Each sample was quenched with THF, and then cooled down in a water bath until room temperature was reached. Any remaining reagent or organic by-products was removed by several successive washing/sedimentation steps using 1) THF, 2) ethanol and 3) acetone, and

4

91   with the help of a centrifuge. The modified particles were then dialyzed in water for two days

92   using a 1 kDa regenerated cellulose membrane and changing the water bath two times a day,

93   to remove the K_2CO_3 catalyst. Finally, the particles were re-dispersed by sonication and

94   freeze-dried.

95   *2.3 Fourier Transform Infrared Spectroscopy (FT-IR)*

96   1-2 wt. % of modified CNC was grinded in a KBr matrix, then pressed under 200 bars for

97   5 min to form a pellet. The spectra were recorded on a Fourier Transform Infrared Bruker

98   spectrometer in transmission mode. Spectra were recorded between 4000 and 400 cm^{-1}, with a

99   resolution of 4 cm^{-1}, and using 64 scans. The spectra were assigned to the same baseline and

100   normalized on the C-O stretching vibration of the glucopyranose ring of cellulose at 1060 cm^{-1}

101   .

102   *2.4 Solid-state ^{13}C CP-MAS NMR spectroscopy*

103   ^{13}C magic angle spinning (MAS) NMR measurements were performed on a 500 MHz

104   Bruker Avance II NMR spectrometer WB (Wissembourg, France), working at frequency of

105   125.8 MHz (4 mm dual CPMAS (1H/BB)). Samples were placed into 4 mm Zirconia rotors

106   (Cortecnet, Paris) of various volumes (70 to 90 μL), closed with a Kel-F cap, then spun at the

107   magic angle frequency set to 10 kHz. All spectra were recorded using a cross polarization,

108   CP, pulse sequence with a two-pulse phase modulation (TPPM) proton decoupling and with a

109   recycling delay of 5 s at 298 K. An average of 2000 scans was collected for each spectrum

110   and a Lorentzian filtering function of 3 Hz was applied. ^{13}C chemical shifts are reported

111   relative to the glycine external reference, whose carbonyl group was set at 176.03 ppm.

112   *2.5 Elaboration of the Pickering emulsions*

113   CNCs grafted with alkyl linear chains varying in lengths (from C2 to C18) and surface

114   degree of substitution (DS_{surf} = 0.04 to 0.66) were dispersed at the required concentration in

115 the continuous phase, being water or hexadecane according to the emulsion type. Two ml of

116 the different Pickering emulsions were prepared, with a W/O ratio of 80/20 v/v for direct

117 emulsions and 20/80 v/v for inverse emulsions. The amount of CNCs was adjusted to reach a

118 concentration of 8 mg of modified CNC per ml of oil phase (i.e. 3.2 and 12.8 mg of CNCs for

119 the 80/20 and 20/80 ratios, respectively). For direct emulsions, 0.4 mL of hexadecane was

120 added to 1.6mL of aqueous suspension of modified CNCs containing 50 mM NaCl. For

121 inverse emulsions, the modified CNCs were dispersed in hexadecane and 0.4 mL of water

122 containing fluorescein and 50 mM NaCl was added. In both cases, the mixture was then

123 sonicated with an ultrasonic device equipped with a dipping titanium probe (QSonica Q700,

124 150 J by alternating 2 s sonication with a 1 s standby for a total of 60 s).

125 *2.6 Determination of the emulsion type using fluorescence microscopy*

126 The emulsions were systematically visualized by transmission optical microscopy with

127 fluorescence detection in order to determine the type of emulsion formed (direct or inverse).

128 A total of 5 μL of the resulting Pickering emulsion was poured onto a slide with spacer and

129 observed with a BX51 Olympus microscope.

130 *2.7 Droplet size analyses with increasing concentrations of grafted CNCs*

131 The droplet diameters distributions were measured by laser light scattering using a

132 Horiba LA-960 particle size distribution analyzer (Kyoto, Japan) for the different modified

133 CNCs at concentrations ranging from 0.4 to 16 mg of CNCs per ml of dispersed phase in the

134 range 0.01–5000 μm. An analysis model was used with refractive index of 1.43 and 1.33 for

135 hexadecane and water, respectively. Measurements were carried out on direct emulsions only.

136 Depending on the samples, 50 to 200 μl of the emulsions were introduced into the cell in

137 order to reach a transmittance around 95–97%. The alignment was performed before each

138 measurement and data acquisition times were set as default. The measurements were

139 systematically carried out in triplicate. The diameter was expressed as surface mean diameter

140   D(3,2) (Sauter diameter). The surface coverage (C) was determined from the ratio of

141   theoretical maximum surface area susceptible to be covered by the particles Sp, and the total

142   surface displayed by the radius of the oil droplets Sd (Kalashnikova, Bizot, Cathala, &

143   Capron, 2011):

144 $$C = {S_p}/{S_d} = \frac{m_p D}{6 h \rho V_{oil}} \qquad \text{Eq. 1}$$

145   where m_p is the mass of CNCs introduced per mL of the dispersed phase, D is the sauter

146   mean diameter of the droplets (also called $D_{3,2}$), h is the thickness defined by AFM, ρ is the

147   CNCs density (1.6 g/cm^3) and V_{oil} is the volume of oil included in the emulsion after

148   centrifugation.

7

3. Results and discussion

3.1 Chemical modification of the CNCs

The cellulose nanocrystals (CNCs) used in this study were obtained by sulphuric acid hydrolysis of wood pulp. They consist of negatively charged rod-like particles (Zeta potential of -51 ± 6 mV) with dimensions of 110 ± 48 nm in length and 4.8 ± 1.1 nm in thickness as determined by atomic force microscopy (Brand, Pecastaings, & Sèbe, 2017; Dhuiège, Pecastaings, & Sèbe, 2019). The amount of hydroxyl groups at their surface was estimated at a value of 3.1 ± 0.1 mmol.g^{-1}, which corresponds to 16.7 % of the total number of OH groups found in the particle (Brand, Pecastaings, & Sèbe, 2017). From this material, amphiphilic CNCs were produced by substituting some of the hydrophilic surface hydroxyl groups by hydrophobic acyl moieties, through an acylation reaction based on the transesterification of vinyl esters and catalyzed by potassium carbonate (Fig. 1). During the reaction, the released vinyl alcohol tautomerizes quickly to acetaldehyde, shifting the equilibrium towards the formation of the acylated product (Brand, Pecastaings, & Sèbe, 2017). The hydrophilic/hydrophobic balance at the CNCs surface was then finely monitored by varying i) the chain length of the grafted acyl moieties (from C2 to C18) and ii) the reaction time.

170
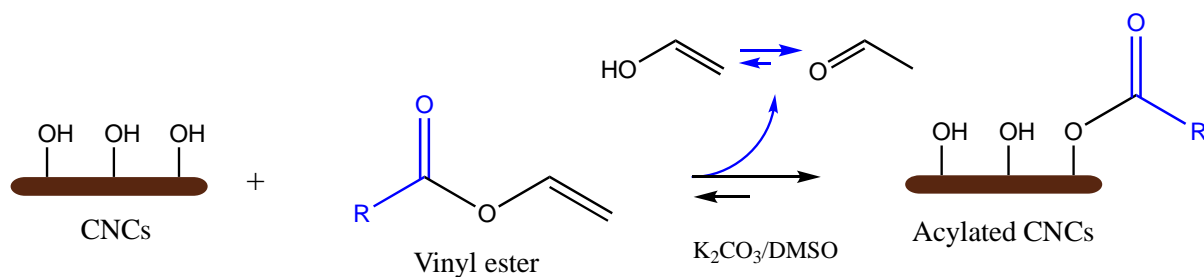
171 R = -CH$_3$ (CNC-Ac/C2), -CH$_2$CH$_3$ (CNC-Pro/C3), -CH$_2$CH$_2$CH$_3$ (CNC-But/C4), -
172 CH$_2$[CH$_2$]$_3$-CH$_3$ (CNC-Hex/C6), -CH$_2$[CH$_2$]$_5$-CH$_3$ (CNC-Oct/C8), -CH$_2$[CH$_2$]$_7$CH$_3$ (CNC-
173 Dec/C10), -CH$_2$[CH$_2$]$_9$CH$_3$ (CNC-Lau/C12), -CH$_2$[CH$_2$]$_{11}$CH$_3$ (CNC-Myr/C14), -
174 CH$_2$[CH$_2$]$_{13}$CH$_3$ (CNC-Palm/C16), -CH$_2$[CH$_2$]$_{15}$CH$_3$ (CNC-Ste/C18)

175 **Fig. 1**. General scheme for the surface acylation of the CNCs with vinyl esters of various

176 chain lengths (in brackets: nomenclature of the sample/number of carbons in the

177 corresponding grafted chain).

178   The efficiency of the reaction was confirmed by observing the characteristic vibrations

179 and chemical shifts of the grafted acyl moieties in the FT-IR and ^{13}C CP-MAS NMR spectra

180 of the modified material (Fig. 2 and 3, respectively). In the FT-IR spectra, the stretching

181 vibration of the carbonyl bond emerges at 1740 cm^{-1} ($\nu_{C=O}$), while the C-H stretchings of the

182 CH$_2$ and -CH$_3$ groups are observed at 2925 and 2850 cm^{-1}. The C-O stretching of the ester

183 bond is also observed at 1230 cm^{-1} in the case of the acetylated sample (CNC-Ac).
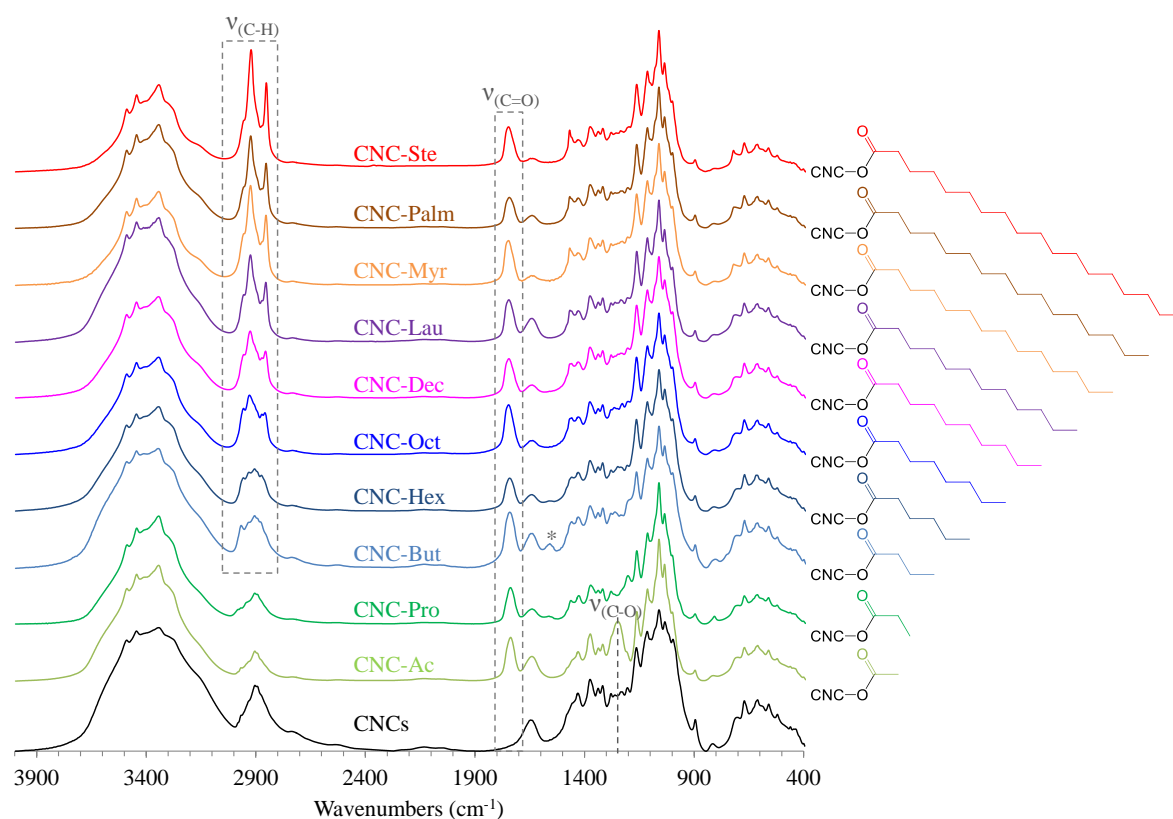
184

Fig. 2. FTIR spectra of the unmodified and acylated CNCs after 5h of reaction. Traces of remaining potassium carbonate catalyst were sometimes observed (*).

In the ^{13}C CP-MAS NMR spectra (Fig. 3), the carbons of cellulose resonate at 110 ppm (C_1), 94 ppm (C_4 crystalline), 89 ppm (C_4 amorphous), 77-80 ppm (C_2, C_3 and C_5), 70 ppm (C_6 crystalline) and 68 ppm (C_6 amorphous) (Attala, Gast, Sindorf, Bartuska, & Maciel, 1980), while the grafted moieties can be seen at 175 ppm (signal of the carbonyl) and in the 10-40 ppm region (signals of the methylene and methyl carbons). Whatever the sample, the NMR cellulose pattern was not modified by the acylation treatment and the signals corresponding to the crystalline domains retained their sharpness, which is consistent with a grafting limited to the outer surface of the nanoparticles.
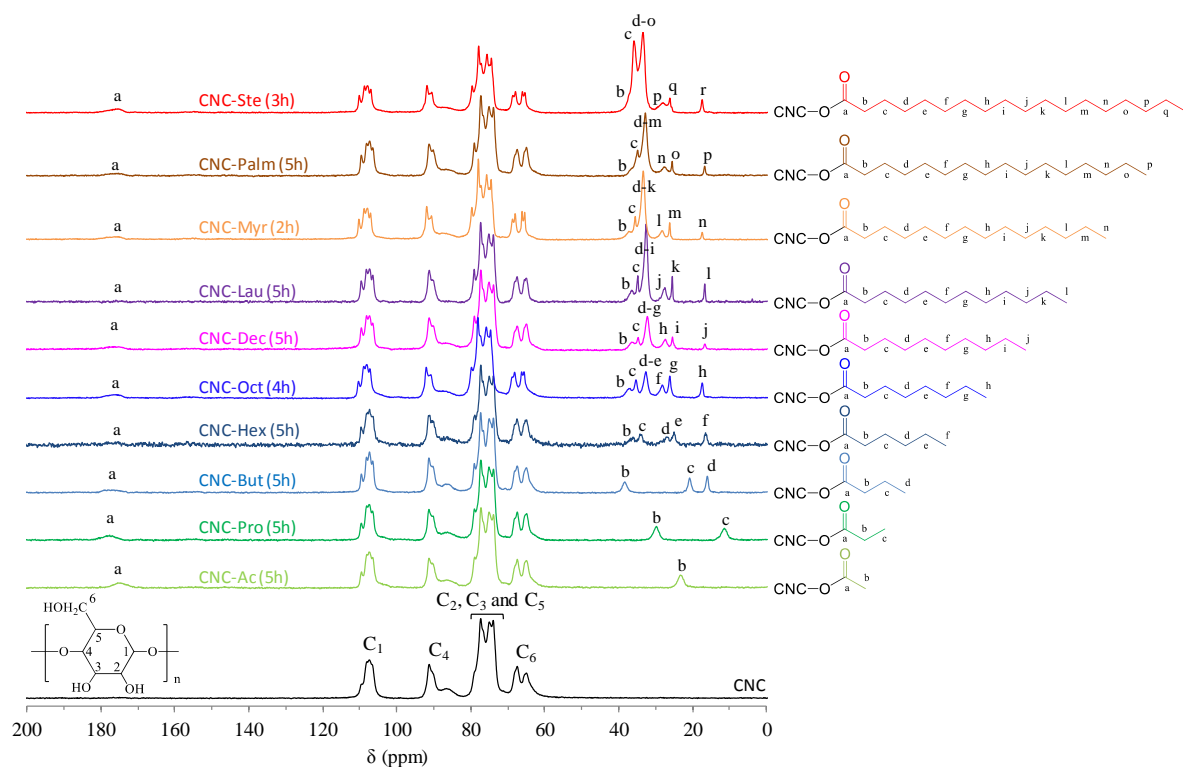
Fig. 3. ^{13}C solid-state CP-MAS NMR spectra of the unmodified and acylated CNCs, with the assignment of the characteristic signals (reaction time in brackets).

The average degree of substitution (DS) per anhydroglucose unit (AGU) was deduced from the NMR spectra, by comparing the average integral per carbon for the grafted chain (between 0 and 40 ppm and at 180 ppm), with the integral of the C_1 carbon of cellulose used as reference:

$$DS = \frac{\text{Sum of the intregrals for the grafted chain/number of carbons in the chain}}{\text{Integral of the C1 of cellulose}} \qquad \text{Eq. 2}$$

This DS was later converted into a surface degree of substitution (DS_{Surf}), knowing that only 16.7 % of the hydroxyl groups – i.e. 33.4 % of the total AGU – are located at the surface of the CNCs and hence accessible for a chemical reaction (Brand, Pecastaings, & Sèbe, 2017):

$DS_{Surf} = DS/0.334.$ Eq. 3

11

208   As only 1.5 OH per AGU (in average) is truly accessible at the surface (Eyley, &

209   Thielemans, 2014), the maximum value that the DS_{Surf} can reach is 1.5 (which is attained

210   when all the surface OH groups are substituted). The extent of surface grafting over time was

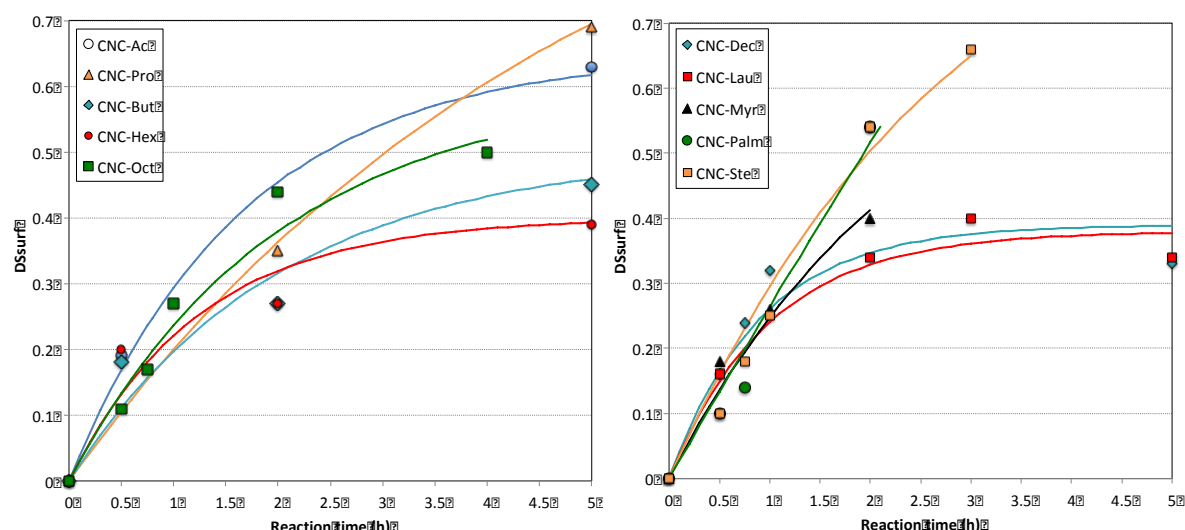211   then quantified for each treatment, by plotting the DS_{Surf} as a function of reaction time

212   (Fig. 4).

213

214   **Fig. 4.** Evolution of the DS_{Surf} as a function of reaction time for the different acylated

215   samples.

216   The reaction kinetics were quite similar for all treatments during the first hour (DS_{Surf} =

217   0.2-0.3 after 1 h), but discrepancies were increasingly noted as the reactions further

218   proceeded. In most cases, a DS_{Surf} of 0.4-0.5 was reached after 2 to 5 h of reaction, but a

219   number of samples displayed a higher modification rate, namely CNC-Ac, CNC-Pro, CNC-

220   Palm and CNC-Ste (DS_{Surf} = 0.5 to 0.7). The higher reactivity of the corresponding vinyl

221   esters has not been explained at this stage of the study (the reactivity is obviously not simply

222   related to the bulkiness of the reactant). The O_3 hydroxyl being involved in the strong O_3-

223    $H^{...}O_5$ intrachain hydrogen bond (Eyley, & Thielemans, 2014), the reactivity of the hydroxyl

224   groups at the cellulose surface should decrease in the order $O_6 \geq O_2 > O_3$, as was observed in

225   the case of the heterogeneous acetylation of cellulose (Goodlett, Dougherty, & Patton, 1971).

226   Due to bulkiness of most vinyl esters, it is also likely that only the O_6 hydroxyl is modified

227   when the DS_{Surf} is below 0.5 (i.e. when less than one third of the surface OH groups are

228   modified). Above this value, some O_2 hydroxyls should start to be acylated. In any case, the

229   different treatments performed here allowed obtaining a wide variety of amphiphilic CNCs

230   grafted with chains of various lengths (from C2 to C18) and various surface degree of

231   substitution (DS_{surf} = 0.1 to 0.7), which were used as model Pickering particles in subsequent

232   investigations.

233   *3.2 Impact of grafting on direct O/W emulsions*

234   In a first set of experiments, various emulsions were prepared by sonicating the CNCs

235   aqueous suspensions with hexadecane, at a W/O volume ratio of 80/20, and observed after

236   24h. The type of emulsion (O/W or W/O) was inferred by pouring a drop of emulsion in a

237   volume of either hexadecane or water (Fig S1 in Supplementary Material). In these

238   conditions, stable O/W emulsions were systematically obtained with the particles grafted with

239   short acyl chains (C2 to C6), regardless of the DS_{surf}. For chains with more than 8 carbons,

240   dense and resistant O/W emulsions could be produced only when the DS_{surf} was $\leq$ 0.15, the

241   emulsions being unstable at higher DS_{surf} (Fig. 5). This behavior is directly linked to the high

242   hydrophobicity of the acyl groups of 8 carbons or more, which confer an excessive

243   hydrophobicity to the particles when DS_{surf} > 0.15, leading to unstable direct O/W emulsions

244   (Binks, & Lumsdon, 2000).

245

	10'	15'	30'	45'	1H	2H
C8	$DS_{surf} = 0.04$	$DS_{surf} = 0.07$	$DS_{surf} = 0.13$	$DS_{surf} = 0.19$	$DS_{surf} = 0.24$	$DS_{surf} = 0.38$
C10	$DS_{surf} = 0.06$	$DS_{surf} = 0.09$	$DS_{surf} = 0.16$	$DS_{surf} = 0.22$	$DS_{surf} = 0.26$	$DS_{surf} = 0.35$
C12	$DS_{surf} = 0.05$	$DS_{surf} = 0.08$	$DS_{surf} = 0.15$	$DS_{surf} = 0.20$	$DS_{surf} = 0.24$	$DS_{surf} = 0.33$
C14	$DS_{surf} = 0.04$	$DS_{surf} = 0.07$	$DS_{surf} = 0.14$	$DS_{surf} = 0.19$	$DS_{surf} = 0.25$	$DS_{surf} = 0.41$
C16	$DS_{surf} = 0.04$	$DS_{surf} = 0.07$	$DS_{surf} = 0.13$	$DS_{surf} = 0.20$	$DS_{surf} = 0.26$	$DS_{surf} = 0.52$
C18	$DS_{surf} = 0.05$	$DS_{surf} = 0.08$	$DS_{surf} = 0.16$	$DS_{surf} = 0.23$	$DS_{surf} = 0.30$	$DS_{surf} = 0.50$

246

Fig. 5. Pictures of the hexadecane-in-water emulsions stabilized by the CNCs modified with long acyl chains (C8 to C18) and various DS_{surf} (obtained after 10', 15', 30', 45', 1h and 2h of reaction), observed after 24h of storage at room temperature (W/O ratio = 80/20 v/v). The DS_{surf} estimated from the trend curves in Fig. 4 are also reported.

The CNCs concentration dependence on the average drop diameter of the direct O/W emulsions was determined for the different CNC samples. When the concentration of native CNCs was increased from 0.1 to 4 g/L in the aqueous phase, the droplet diameter of the emulsion decreased until reaching a plateau at 3µm (Fig. 6). This behavior is in accordance with the so-called limited coalescence process (Arditty, Whitby, Binks, & Leam-Calderon, 2003). After sonication, the uncovered droplets merge; this coalescence is stopped when the

257   minimum drop coverage required for stability is reached. The drop diameter depends then

258   directly on the amount of particle available to stabilize the interface. The second part of the

259   curve presents a plateau. It occurs when the drop diameter cannot decrease anymore; the

260   system will evolve at constant interface area. In many systems, the particles are released in

261   the continuous phase but rods can move at the interface and orientate into parallel bundles

262   leading to densification of the CNC organization (Cherhal, Cousin, & Capron, 2016). The

263   same profile was observed in Fig. 6 for CNCs modified with short acyl chains (from C2 to

264   C6), but differences were noted with the CNCs grafted with longer hydrophobic chains ($\geq$

265   C8). For these samples, a higher droplet diameter is observed at a given particles

266   concentration and degree of substitution, as well as a shift in the concentration needed to

267   reach the plateau at 3µm (Fig. 6). The limited coalescence domain is controlled by the

268   irreversible adsorption of particles at the interface. When the surface is totally covered, a

269   plateau in drop diameter is observed. The limit concentration between these two domains was

270   evaluated at 0.5 g/L for unmodified CNCs, 2 g/L for the CNCs grafted with C2 to C8, and

271   more than 4 g/L for those grafted with C10. Hence, there is a clear impact of chain length on

272   the stabilization process for direct O/W emulsions, which could result from an increasing

273   aggregation of the CNCs at the droplets surface, through hydrophobic interactions, leading to

274   a decrease of the total surface available for the stabilization of the O/W interface.

275   A similar result was obtained when the hydrophobicity at the surface of the particles was

276   progressively increased with a single acyl group, through the incrementation of the DS_{Surf}

277   (Fig. 7a). To further evaluate the organization of the particles at the interface, the coverage

278   percentage (C) for the various samples was estimated with Eq. 1, from the slope of the

279   reciprocal surface-average diameter (1/D) plotted as a function of CNCs concentration (for

280   direct emulsions, and expressed in mg per ml of oil phase) (Fig. 7b). The coverage ratio

281   decreases progressively from a fully covered surface with a value of 107 %, to a slightly

282   covered surface with a value of 27% when the DS_{surf} increased from 0 to 0.19 respectively,

283   confirming the enhanced aggregation state of the CNCs at higher modification rate. A similar

284   aggregation has been reported in the literature after reduction of the electrostatic repulsions

285   between native CNCs, through desulfatation of their surface (Cherhal, Cousin, & Capron,

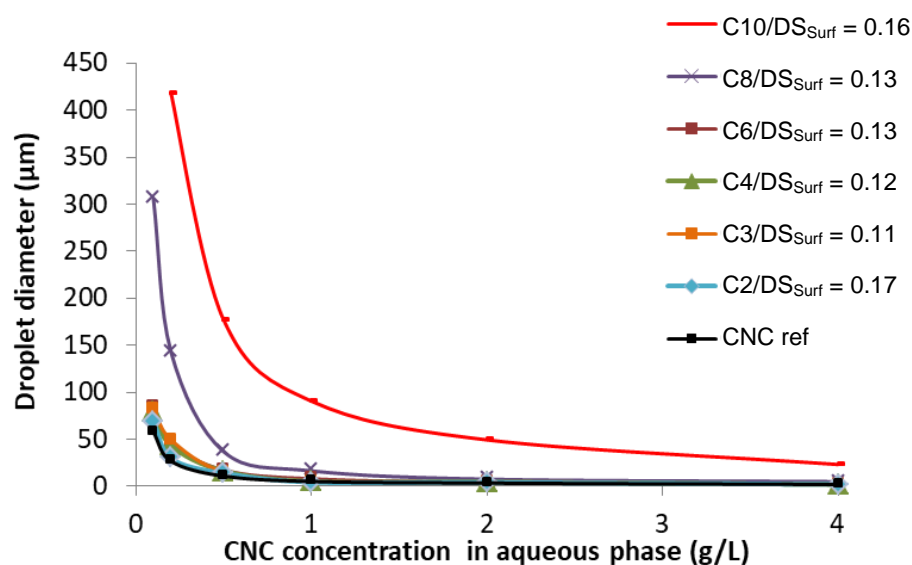286   2016), leading to a more porous and heterogeneous droplet surface.

287

288   **Fig. 6.** Evolution of the direct emulsion droplet diameter with increasing particles

289   concentration for CNCs grafted with acyl chains of C2 to C10, with a DS_{Surf} in the same order

290   of magnitude (the DS_{surf} was estimated from the trend curves in Fig. 4).
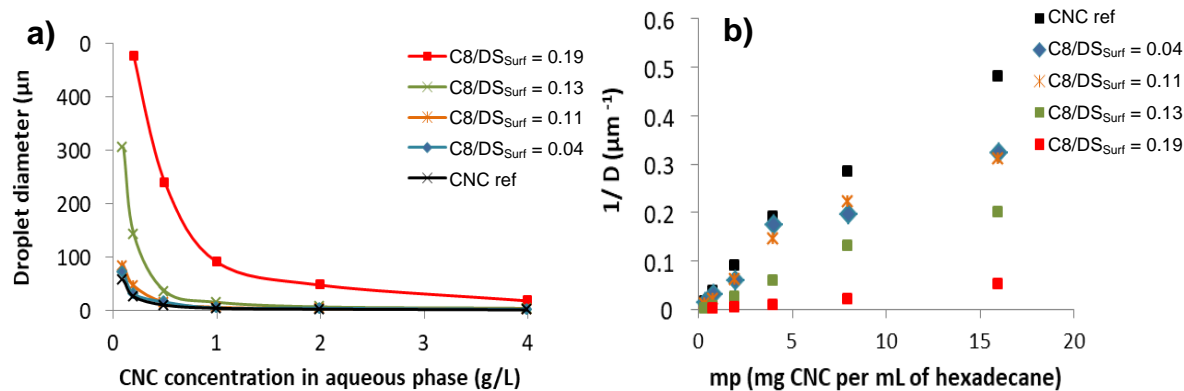
291

292

293

Fig. 7. a) Evolution of the direct emulsion droplet diameter with increasing particles concentration for the CNCs grafted with C8 acyl chains of various DS_{Surf} (the DS_{surf} was estimated from the trend curves in Fig. 4). **b)** Inverse D(3,2) diameter plotted as a function of particles concentration (expressed in mass of CNCs per mL of hexadecane).

All the O/W emulsions were further confirmed by staining the water continuous phase with fluorescein (appearing in green) and visualizing the droplets with a fluorescence microscope. Some typical results are exemplified in Fig. 8. The CNCs grafted with short acyl chains (C2 to C6, regardless of the DS_{surf}), or long chains and low DS_{surf} (C8 to C18 and $DS_{surf} \leq 0.15$), led to O/W emulsions with small oil droplets (about 3 μm) and low size distributions in the images (Fig. 8A-B). The oil droplets that are creaming can be seen in black in contact with the slide in Fig. 8B, while the continuous phase appears clearly in green.
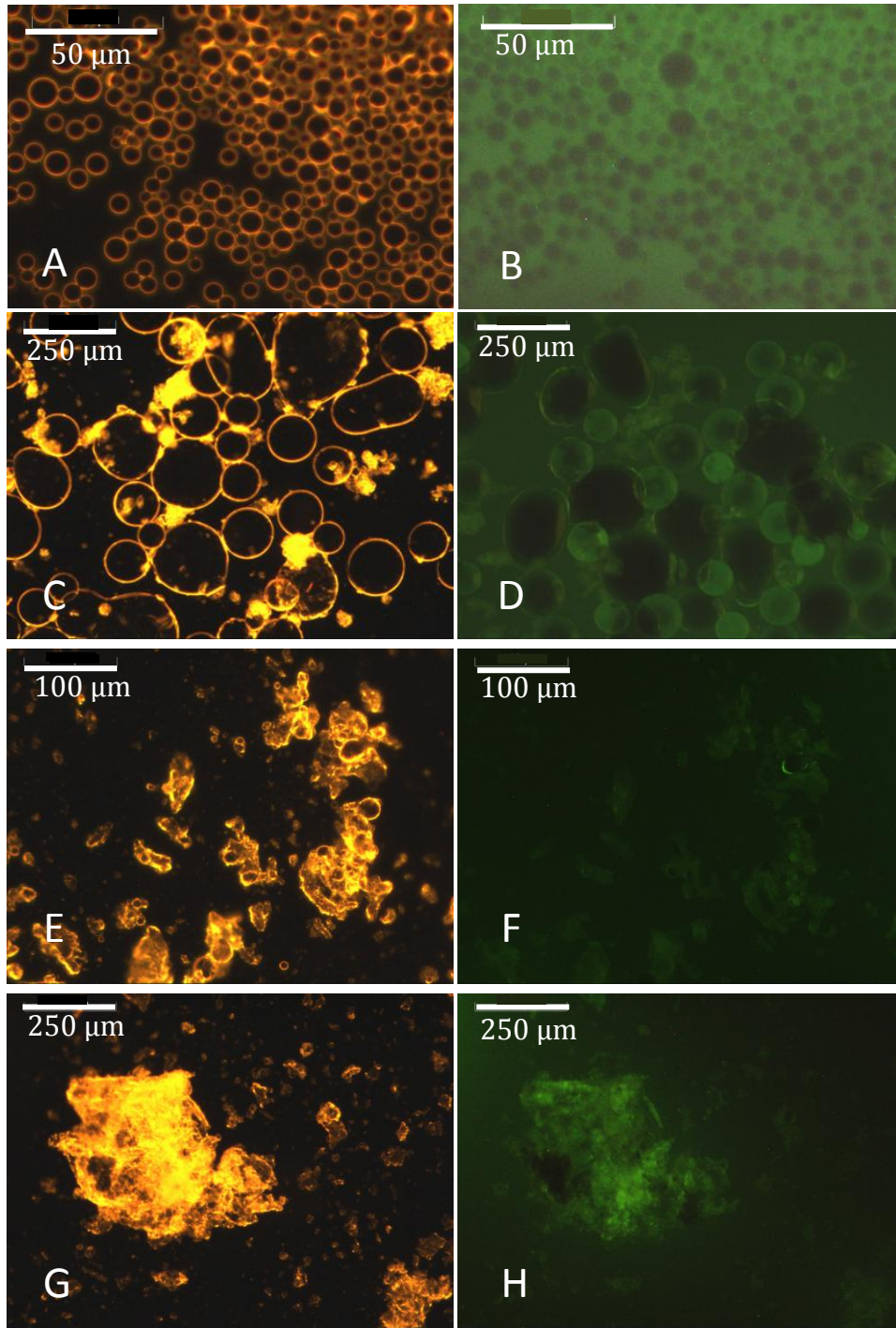
17

310

Fig. 8. Optical (A, C, E, G) and fluorescence (B, D, F, H) microscopy images of a typical (A-B) direct O/W emulsion (here: C8-graft with $DS_{surf} = 0.13$), (C-D) intermediate state where oil droplets co-exist with aggregated water droplets (here: C8-graft with $DS_{surf} = 0.24$), and (E-H) inverse W/O emulsion (here: C8-graft with $DS_{surf} = 0.38$).

315

3.3 Inverse W/O emulsions

317   In a second set of experiments, emulsions were prepared by dispersing the hydrophobized

318   CNCs in the oil phase, then sonicating the suspension with a lower volume of water (W/O =

319   20/80 v/v), with the objective to produce inverse emulsions. Here again, the type of emulsion

320   was inferred by observing what happens when a drop of emulsion was added to a volume of

321   either hexadecane or water (Fig. S1 in Supplementary Material). In these conditions, only the

322   particles grafted with acyl chains of 8 carbons or more produced inverse W/O emulsions, and

323   only when the particles surface was sufficiently modified (i.e. when DS_{surf} was above 0.2-0.3,

324   depending on the acyl chain). The formation of W/O emulsions with the longer acyl chains

325   was further confirmed by fluorescence microscopy, the water encapsulated in the oil phase

326   appearing in the form of various irregular structures that may correspond to coalesced water

327   droplets (Fig. 8E-G and Fig. S2 in Supplementary Material). It has been indeed shown in a

328   comprehensive study by Simovic & Prestige 2004, that for hydrophobic nanoparticles coated

329   droplets, the limited coalescence process can result in a flocculated network composed of

330   coalesced droplets of irregular shapes. At intermediate DS_{surf}, the microscopy images revealed

331   an intermediate state, where creaming oil droplets seem to co-exist with aggregated water

332   droplets (Fig. 8C-D). These microscopic observations are quite puzzling, but could be related

333   to the co-existence of CNCs of low and high acylation levels when the reaction time is

334   intermediate; the initial cellulosic substrate is indeed quite variable and the calculated DS_{surf}

335   represents only an average estimate. Besides, the oil droplets observed in this intermediate

336   state are larger than those of the direct emulsions, confirming that less low-acylated particles

337   are available to stabilize this interface, some of the particles (the more acylated ones) being

338   probably consumed by the interface of the water droplets seen in the microscopic images.

339   The different types of emulsions obtained in our experiments are summarized in Fig. 9, as

340   a function of chain length (C2 to C18) and surface degree of substitution (DS_{surf} = 0.04 to

341 0.69). These results show that, with the DS_{surf} obtained in our experimental conditions (DS_{surf}

342 $\leq 0,7$), it is never possible to produce inverse emulsions with short alkyl chains (C2 to C6). In

343 the better case, less than 50% of the surface OH groups are substituted (the theoretical

344 maximum DS_{surf} being 1.5), which is too low to impart a sufficient hydrophobicity to the

345 CNCs surface and stabilize W/O emulsions with such short lengths. Distinctively, all the

346 particles grafted with more than 8 carbons allow the stabilization of both direct and inverse

347 emulsions, depending on the level of grafting. If O/W emulsions necessitate low DS_{surf},

348 stabilization of W/O emulsions is possible only when the CNCs surface is sufficiently

349 modified by the long chains. Beyond 8 carbons, inverse emulsions are indeed systematically

350 produced if $DS_{surf} > 0.25$, i.e. when about one third of the surface OH groups are substituted.

351 However, long chains will tend to entangle via hydrophobic interactions, leading to large

352 particles assemblies and low surface coverage of the droplets at the interface; more material is

353 consequently required for an efficient surface stabilization in that case. It can be noted that

354 similar results were obtained when the hexadecane oil was replaced by toluene (results not
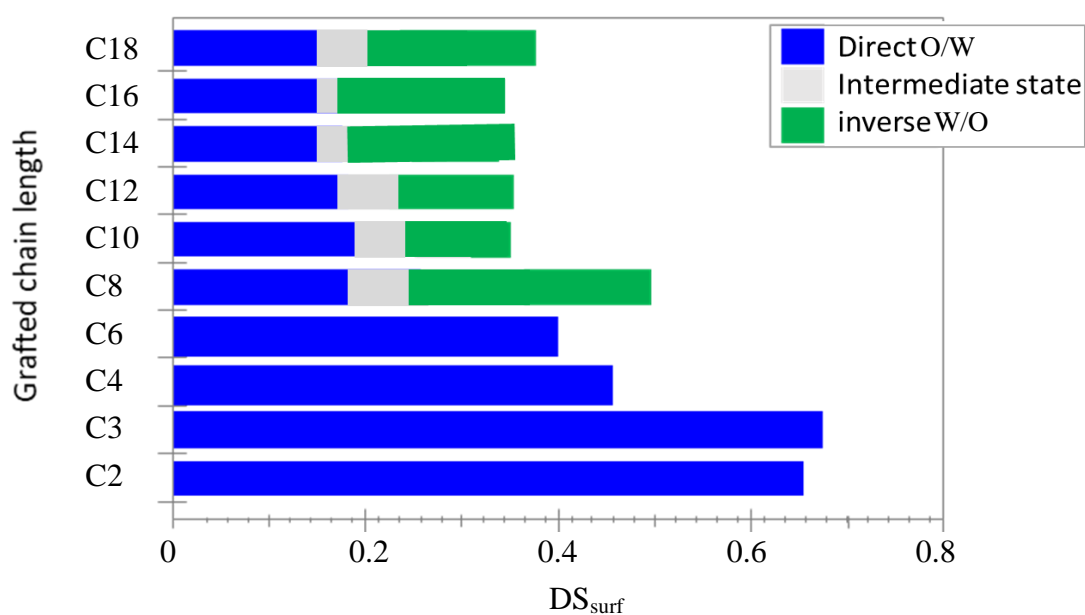
355 shown).

356

357

358

Fig. 9. Type of emulsion obtained in our experimental conditions as a function of DS_{Surf} and number of carbons in the grafted chain. Direct and inverse emulsions are obtained with W/O = 80/20 and 20/80 v/v, respectively. The intermediate state corresponds to a situation where both oil and water droplets are present in the medium according to the microscopic observations.

4. Conclusions

This work investigates the potential of surface acylation as a tool to monitor the properties of Pickering emulsions stabilized by cellulose nanocrystals (CNCs), through the control of the grafted chain length and grafting level. Amphiphilic CNCs grafted with acyl groups of various chain lengths and surface degree of substitution (DS_{surf}) were produced, through an acylation reaction based on the transesterification of vinyl esters. The grafting was confirmed by FT-IR and ^{13}C CP-MAS NMR spectroscopy, and quantified by the calculation of the surface degree of substitution (DS_{surf}) obtained from the NMR spectra. Whatever the DS_{Surf}, CNCs grafted with linear acyl chains of 2 to 6 carbons led to the exclusive formation of direct O/W emulsions with hexadecane. When the linear chain contained 8 carbons or more, both O/W and W/O emulsions could be obtained at low and high DS_{Surf}, respectively. The inverse W/O emulsions could be stabilized only when at least one third of the surface OH groups were substituted. At intermediate DS_{surf}, the microscopic investigations revealed the existence of an intermediate situation where both oil and water droplets seem to co-exist, which could be related to the variability of the acylation process (co-existence of CNCs of low and high acylation levels). The chain length and DS_{Surf} had a clear impact on the stabilization process for direct O/W emulsions, larger droplets being obtained for a given particles concentration at higher chain length and DS_{Surf}. This was assigned to an increasing aggregation of the CNCs at the droplets surface, through hydrophobic interactions, leading to a decrease of the total surface available for the stabilization of the O/W interface. As a consequence, the surface coverage of the emulsion droplets is significantly varied, which should have an impact on the permeability of the Pickering capsules in delivery applications. In any case, we were able to monitor the type of emulsion formed, droplet size and surface coverage at the oil/water interface, by adjusting the length of the grafted chain, DS_{Surf}, and particles concentration.

389

Supplementary material

    Supplementary material related to this article can be found in the online version.

References

Arditty, S., Whitby, C. P., Binks, B. P., Schmitt, V., & Leal-Calderon, F. (2003). Some general features of limited coalescence in solid-stabilized emulsions. *European Physical Journal E,* 11(3), 273-281.

Attala, R. H., Gast, J. C., Sindorf, D. W., Bartuska, V. J., & Maciel, G. E. (1980). Carbon-13 NMR spectra of cellulose polymorphs. *Journal of the American Chemical Soc*iety, 102 (9), 3249-3251.

Belanger, S. E., Dorn, P. B., Toy, R., Boeije, G., Marshall, S. J., Wind, T., Van Compernolle R., & Zeller, D. (2006). Aquatic risk assessment of alcohol ethoxylates in North America and Europe. *Ecotoxicology and Environmental Safety,* 64(1), 85-99.

Binks, B. P., & Lumsdon, S. O. (2000). Influence of Particle Wettability on the Type and Stability of Surfactant-Free Emulsions. Langmuir, 16(23), 8622-8631

Binks, B. P. (2002). Macroporous silica from solid-stabilized emulsion templates. *Advanced Materials,* 14(24), 1824-1827.

411   Brand, J., Pecastaings, G., Sèbe, G. (2017). A versatile method for the surface tailoring of

412   cellulose nanocrystal building blocks by acylation with functional vinyl esters.

413   *Carbohydrate Polymers*, 169, 189-197.

414   Capron, I., Rojas, O. J., & Bordes, R. (2017). Behavior of nanocelluloses at interfaces.

415   *Current opinion in colloid and interface science,* 29, 83-95.

416   Cherhal, F., Cousin, F., & Capron, I. (2016). Structural Description of the Interface of

417   Pickering Emulsions Stabilized by Cellulose Nanocrystals. *Biomacromolecules,* 17(2),

418   496-502.

419   Cunha, A. G., Mougel, J.-B., Cathala, B., Berglund, L. A., & Capron, I. (2014). Preparation of

420   Double Pickering Emulsions Stabilized by Chemically Tailored Nanocelluloses.

421   *Langmuir,* 30(31), 9327-9335.

422   Dhuiège, B., Pecastaings, G., Sèbe, G. (2019). A Sustainable approach for the Direct

423   Functionalization of Cellulose Nanocrystals Dispersed in Water by Transesterification of

424   Vinyl Acetate. *ACS Sustainable Chemistry & Engineering*, 7, 187-196.

425   Eyley, S., & Thielemans, W. (2014). Surface modification of cellulose nanocrystals.

426   *Nanoscale,* 6(14), 7764-7779.

427   Goodlett, V. W., Dougherty, J. T., Patton, H. W. (1971). Characterization of cellulose acetates

428   by nuclear magnetic resonance. *Journal of Polymer Science Part A-1: Polymer*

429   *Chemistry*, 9, 155–161.

430   Habibi, Y. (2014). Key advances in the chemical modification of nanocelluloses. *Chem Soc*

431   *Rev,* 43, 1519-1542.

432   Habibi, Y., Lucia, L. A., & Rojas, O. J. (2010). Cellulose Nanocrystals: Chemistry, Self-

433   Assembly, and Applications. *Chemical Reviews,* 110(6), 3479-3500.

434   Kalashnikova, I., Bizot, H., Cathala, B., & Capron, I. (2011). New Pickering Emulsions

435   Stabilized by Bacterial Cellulose Nanocrystals. *Langmuir,* 27(12), 7471-7479.

436   Kalashnikova, I., Bizot, H., Cathala, B., & Capron, I. (2012). Modulation of Cellulose

437   Nanocrystals Amphiphilic Properties to Stabilize Oil/Water Interface.

438   *Biomacromolecules,* 13(1), 267-275.

439   Lee, K.-Y., Blaker, J. J., Murakami, R., Heng, J. Y. Y., Bismarck, A. (2014). Phase Behavior

440   of Medium and High Internal Phase Water-in-Oil Emulsions Stabilized Solely by

441   Hydrophobized Bacterial Cellulose Nanofibrils, *Langmuir*, 30 (2), 452−460.

442   Moon, R. J., Martini, A., Nairn, J., Simonsen, J., & Youngblood, J. (2011). Cellulose

443   nanomaterials review: structure, properties and nanocomposites. *Chemical Society*

444   *Reviews,* 40(7), 3941-3994.

445   Pickering, S. U. (1907). Emulsions. *Journal of Chemical society* 91, 2001-2021.

446   Sèbe, G., Ham-Pichavant, F., Pecastaings, G. (2013). Dispersibilityand Emulsion-Stabilizing

447   Effect of Cellulose Nanowhiskers Esterified by Vinyl Acetate and Vinyl Cinnamate.

448   *Biomacromolecules*, 14 (8), 2937−2944.

449   Simovitc, S., Prestidge, C. A. (2004). Nanoparticles of varying hydrophobicity at the

450   emulsion droplet-water interface: adsorption and coalescence stability. *Langmuir*, 20,

451   8357-8365.

452   Werner, A., Schmitt, V., Sèbe, G., Heroguez, V. (2017). Synthesis of surfactant-free micro-

453   and nanolatexes from Pickering emulsions stabilized by acetylated cellulose nanocrystals.

454   *Polymer Chemistry,* 17, 8 (39), 6064−6072.

455   Werner, A., Sèbe, G., Héroguez, V. (2018). A new strategy to elaborate polymer composites

456   via Pickering emulsion polymerization of a wide range of monomers. *Polymer*

457   *Chemistry*, 9, 5043-5050.

458   Werner, A., Schmitt, V., Sèbe, G., Héroguez, V. (2019). Convenient synthesis of hybrid

459   polymer materials by AGET-ATRP polymerization of Pickering emulsions stabilized by

460   cellulose nanocrystals grafted with reactive moieties. *Biomacromolecules*, 20, 490-501.

461   Xhanari, K., Syverud, K., Stenius, P. (2011). Emulsions stabilized by microfibrillated

462   cellulose: The effect of hydrophobization, concentration and o/w ratio, *Journal of*

463   *Dispersion Science & Technology*. 32 (3) 447– 452.

464   Zhang, Z., Tam, K. C., Wang, X., Sèbe, G. (2018). Inverse Pickering emulsions stabilized by

465   cinnamate modified cellulose nanocrystals as templates to prepare silica colloidosomes.

466   *ACS Sustainable Chemistry & Engineering*, 6, 2583-2590.

467

468

469

470

471

472

473

474